Manuscript prepared for Atmos. Chem. Phys.
with version 2.3 of the LaTeX class copernicus.cls.
Date: 16 June 2009

Long-lived halocarbon trends and budgets from atmospheric chemistry modelling constrained with measurements in polar firn Supplement

P. Martinerie[1], E. Nourtier-Mazauric[1], J.-M. Barnola[1], W. T. Sturges[2], D. R. Worton[2,*], E. Atlas[3], L. K. Gohar[4,], K. P Shine[4], and G. P. Brasseur[5]**

[1]Laboratoire de Glaciologie et Géophysique de l'Environnement (UMR CNRS/INSU 5183), CNRS, Université Joseph Fourier-Grenoble, BP 96, 38 402 Saint Martin d'Hères, France
[2]School of Environmental Sciences, University of East Anglia, Norwich, NR4 7TJ, UK
[3]Rosenstiel School of Marine and Atmospheric Science, University of Miami, Miami, FL 33149, USA
[4]Department of Meteorology, University of Reading, Reading RG6 6BB, UK
[5]National Center for Atmospheric Research, Boulder, CO 80307-3000, USA
[*]Now at Department of Environmental Sciences, Policy and Management, University of California, Berkeley, CA 94720-3110, USA
[**]Now at Met. Office Hadley Centre, FitzRoy Road, Exeter. EX1 3PB, UK

1 Introduction

This electronic supplement aims at providing additional results from our modelling study. Sections 2, 3 and 4 discuss firn diffusivities, relative diffusion coefficients (D_{gas}/D_{CO_2}) and firn ages in terms more firn-oriented than atmosphere-oriented. Sections 5 and 6 complete some results that are presented in the article only for selected species.

2 Firn diffusivities

Firn diffusivities were re-calculated for this study (see Sect. 5 of the article) using the minimization technique described in Rommelaere et al. (1997). The control method used in inverse modelling aims at minimizing errors, in particular the differences between observations and model estimations of mixing ratios in the firn. The algorithm takes into account a "regularization parameter" (Rommelaere, 1997) which allows to constrain the rugosity of the solution. High values of the regularization parameter were used, leading to less oscillations in the solution and thus smoother diffusivity profiles than those used in previous FIRETRACC and CRYOSTAT publications (FIRETRACC, 2007; CRYOSTAT, 2007). Our diffusivity profiles were calculated using carbon dioxide and methane as reference gases. Methane produces diffusivities which better fit the halocarbon measurements for most sites. This is probably due to the fact that methane is a faster diffusing gas than CO_2, thus its concentrations at the bottom of all firn drilling sites remain far away from its stable pre-industrial level. The diffusivities used in this study (Fig. 1) were thus calculated using CH_4 as reference gas except for Dome C, where methane produces a too steep slope break around 95m depth. It should be due to the fact that the measured methane concentration at 95m depth (Fig. 2) remains close to values at higher depths whereas halocarbon concentrations at 95m depth have begun to drop more significantly. We therefore use the CO_2 derived diffusivity for Dome C.

The comparison of firn model results with CO_2 and CH_4 measured concentrations in firn (Fig. 2) illustrates the fact that uncertainties on diffusivity are higher at the deepest firn levels. At Devon Island, the CO_2 and CH_4 records are inconsistent below 45-50m depth: a diffusivity profile which fits one gas cannot fit the other. The methane derived diffusivity is consistent with halocarbon measurements. The inconsistency between CO_2 and other gases at the bottom of Devon Island firn may be due to the frequent occurrence of melting at this site, which could affect this soluble gas. At North GRIP, the smooth diffusivity profile fails at fitting CO_2 and CH_4 measurements at the two deepest levels. This under-estimation is also observed for halocarbon gases. At all Antarctic sites, CO_2 and CH_4 modelled concentrations continue to decrease importantly after the last measurement. This is related to the steep slopes observed at the bottom of the firn, and to the complete bubble close-off depth which is imposed in the model. Indications about this close-off depth are provided by field data: it is approximately located between the last measurement depth and the depth at which no air could be pumped out of the firn anymore, which represents a one to three meters interval. Our close-off depths were chosen to best fit the data, using this field information. At Berkner Island, the two bottom level measurements (60m and 63m) are suspected of contamination and were not used for diffusivity calculation.

Our firn diffusivities were calculated using the atmospheric trend scenarios for CO_2 and CH_4 described in Fabre et al. (2000). A comparison with scenarios calculated from

Correspondence to: P. Martinerie
(patricia@lgge.obs.ujf-grenoble.fr)

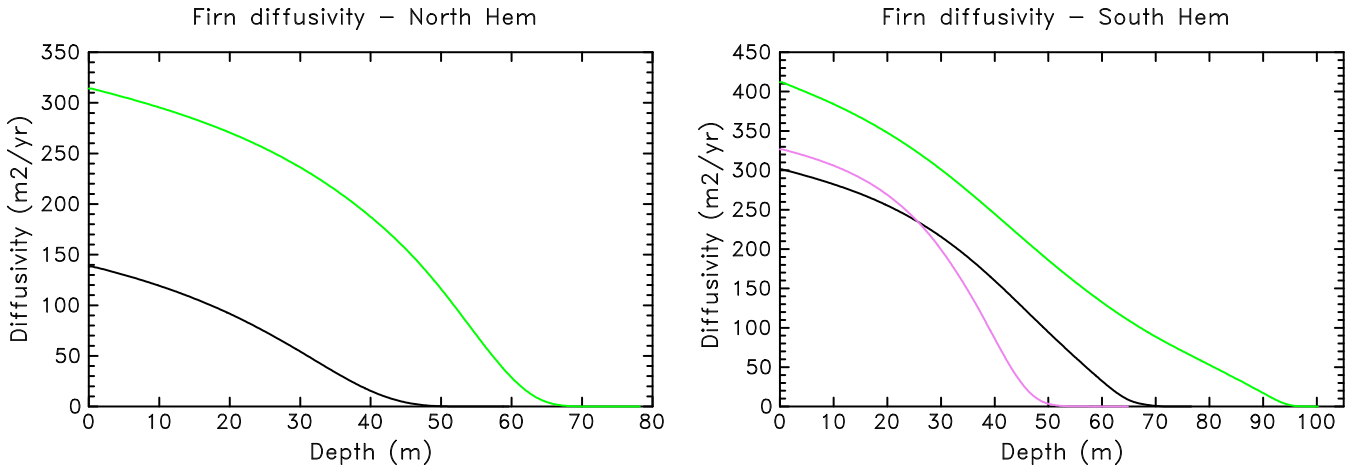

Fig. 1. Firn diffusivities calculated for this study. Left panel: North hemisphere drill sites: Devon Island in black, North GRIP in green. Right panel: South hemisphere drill sites: Berkner Island in violet, Dronning Maud land in black, Dome C in green.

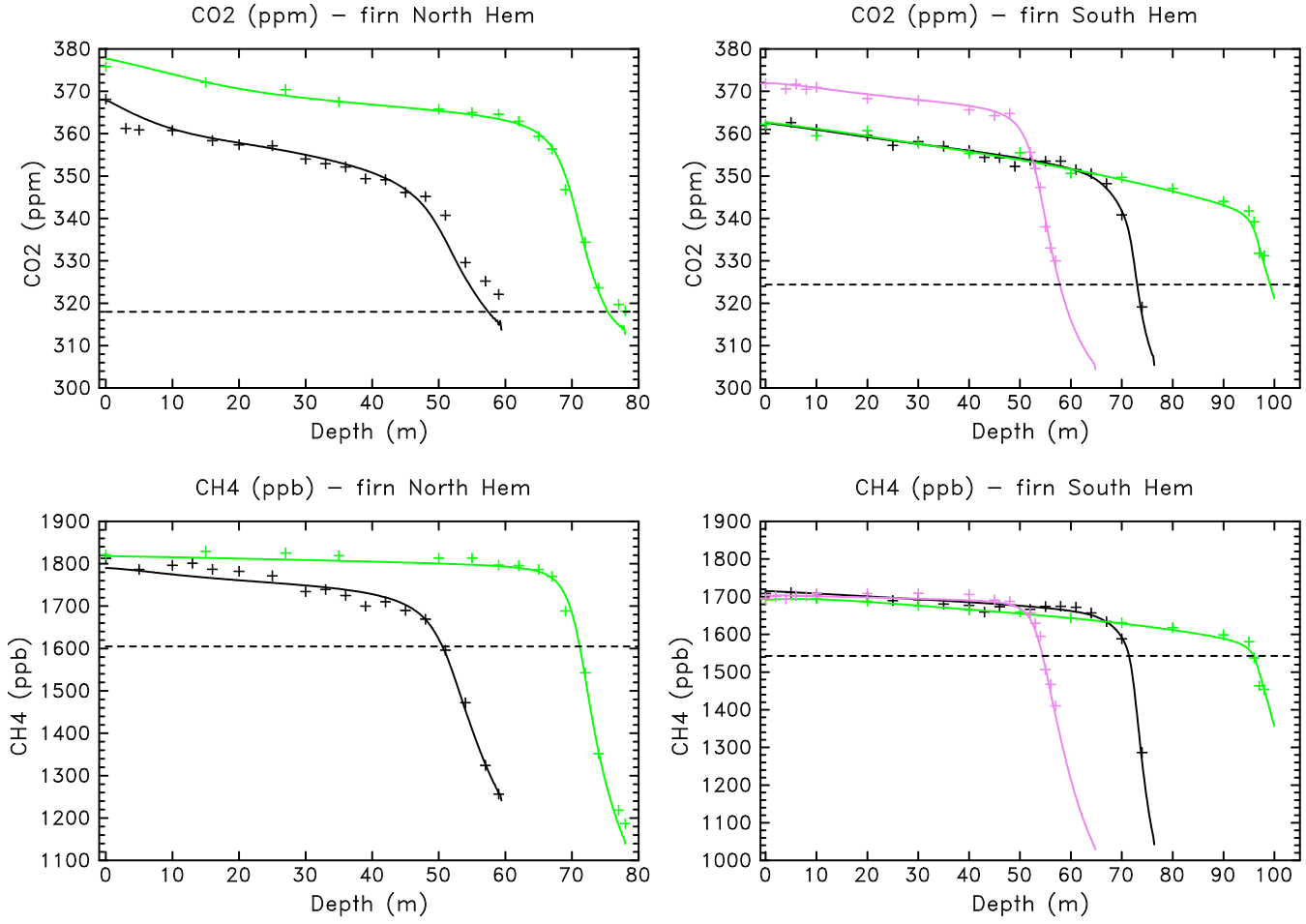

Fig. 2. Comparison of the firn model results (continuous lines) for CO_2 and CH_4 with FIRETRACC and CRYOSTAT data (plus signs). Left panel: North hemisphere drill sites: Devon Island in black, North GRIP in green. Right panel: South hemisphere drill sites: Berkner Island in violet, Dronning Maud land in black, Dome C in green. Horizontal black dashed lines illustrate the lowest atmospheric concentrations measured in the relevant hemisphere. The CO_2 and CH_4 atmospheric trend scenarios were built from a combination of atmospheric, firn and ice core records (Fabre et al., 2000).

Table 1. Molecular diffusion coefficient ratios: values used in this study, comparison with other calculated values and measurements.

D_{gas}/D_{CO_2}	This study	Sturrock et al. (2002)(a) Trudinger et al. (1997)(b)	Matsunaga et al. at 0°C	Matsunaga et al. at -50°C
CFC-11	0.575	0.566 (a)	0.525	0.526
CFC-12	0.618	0.610 (a)	0.592	0.600
CFC-113	0.495	0.486 (a)	0.452	0.453
CFC-114	0.522	0.512 (a)	0.493	0.499
CFC-115	0.554	0.544 (a)	0.529	0.535
CCl_4	0.539	0.530 (a)	-	-
SF_6	0.621	0.583 (b)	0.553	0.556
CH_4	1.415	1.291 (b)	1.370	1.364

the more recent MacFarling Meure et al. (2006) data was performed using the direct firn model. The differences in simulated vertical profiles in firn using the two scenarios do not exceed 0.6 ppm for CO_2 and 33 ppb for CH_4 near the firn-ice transition. These differences are smaller than the experimental uncertainites on the ice-core part of the MacFarling Meure et al. (2006) data. Thus the use of scenarios derived from MacFarling Meure et al. (2006) data for diffusivity calculation is likely to have only a marginal impact on our results.

3 Diffusion coefficients in air

Different trace gases have different diffusion coefficients in air (D_{gas}), which result in different diffusion speeds in firn air. When the firn diffusivity profile is established for a reference gas (e.g. CO_2), it can be applied to another gas by scaling with D_{gas}/D_{CO_2}. Most studies of halocarbons in polar firn (e.g. Butler et al., 1999; Sturges et al., 2000; Sturrock et al., 2002; Trudinger et al., 2002) use calculated values of diffusion coefficients in air based on estimates of halocarbon molecular volumes. Gilliland (1934) expressed diffusion coefficients for binary gas mixtures (D_{AB}) as a function of their molecular masses (M_A, M_B) and volumes (V_A, V_B), temperature (T) and pressure (P):

$$D_{AB} = \frac{\alpha T^{\beta}}{P} \frac{\sqrt{1/M_A + 1/M_B}}{(V_A^{1/3} + V_B^{1/3})^2} \quad (1)$$

with α=0.0043, and β=3/2. For most gases, diffusion coefficients in N_2 and air are similar (e.g. Marrero and Mason, 1972; Matsunaga et al., 1993, 1998). In the theoretical frame of Eq. 1, the D_{gas}/D_{CO_2} diffusion coefficient ratios are independent from temperature and pressure. The diffusion coefficient ratios used in this study for halocarbons (see Table 1) are calculated using atomic volumes from Le Bas (1915) as reported in Perry and Chilton (1973). Diffusion coefficients for CO_2, CH_4 and SF_6 were calculated following Bzowski et al. (1990), as described in Fabre et al. (2000).

Other studies of halocarbons in firn air also use calculated diffusion coefficient ratios. The mostly used methods are from Wilke and Lee (1955) (e.g. in Butler et al. (1999) and Trudinger et al. (1997)), and Fuller et al. (1966) (e.g. in Trudinger et al. (2002) and Sturrock et al. (2002)). Fuller et al. (1966) propose an equation similar to Eq. 1, with different values of α and β and new estimates of atomic and molecular volumes. However, no estimates are provided for the fluorine and bromine atoms. Our values of D_{gas}/D_{CO_2} differ by less than 2% from those used in Sturrock et al. (2002) (Table 1). Higher discrepancies are obtained for CH_4 and SF_6 (6.3% and 9.2% respectively) between our study and Trudinger et al. (1997). Sturrock et al. (2002) estimate the uncertainty on their diffusion coefficient ratios to be about $\pm$ 5%.

A consistent set of diffusion coefficient measurements, not known to have been previously used in firn air studies, has been published for the major greenhouse gases (Matsunaga et al., 1998), CFCs (Matsunaga et al., 1993) and SF_6 (Matsunaga et al., 2002) with experimental precisions of about $\pm$ 2%. A comparison with previous measurements, when available, is provided as well as temperature-dependent equations fitted to the data of the form:

$$D_{AB} = \gamma T^{\delta} \quad (2)$$

where γ and δ are species-dependent scalars. As coefficient δ is species-dependent, the derived D_{gas}/D_{CO_2} ratios are slightly temperature dependent (0.2% to 1.4% in the 0 to -50°C temperature range). Measurements were performed at positive temperatures and are extrapolated to -50°C using Eq. 2 (Table 1). Our calculated diffusion coefficient ratios show larger discrepancies with this experimental data set (3% to 12%) than with theoretical values calculated by Sturrock et al. (2002).

The firn model results obtained with our calculated D_{gas}/D_{CO_2} ratios are compared with results using D_{gas}/D_{CO_2} from (Matsunaga et al., 1993, 1998, 2002) on Figures 3 and 4. The discrepancies are most important for CFC-11, CFC-113 and SF_6, they are increasing with depth and reach about 30% to 40% at the firn-ice transition for these gases. However these discrepancies remain within the uncertainty range due to firn data dispersion, firn diffusiv-

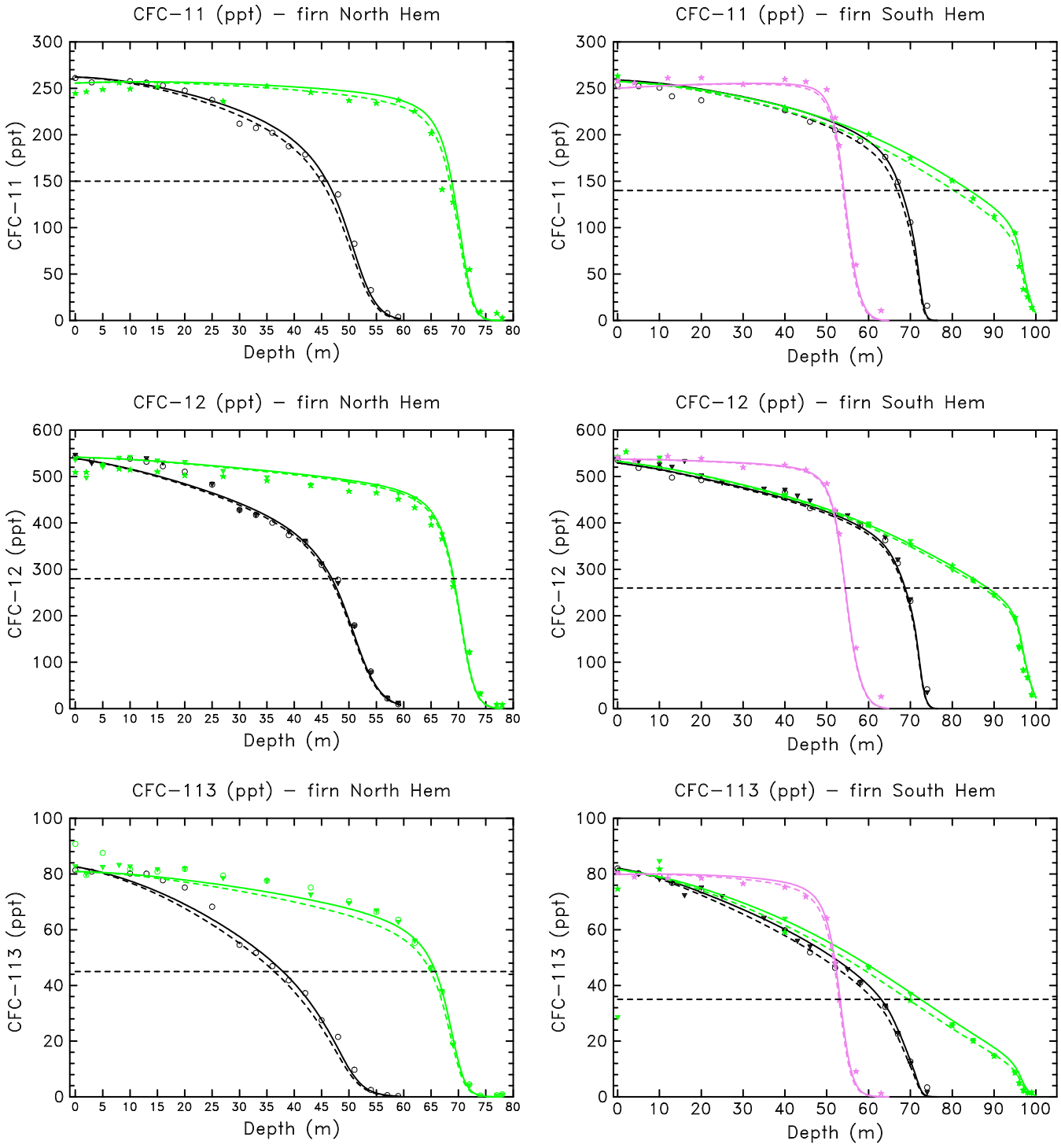

Fig. 3. Comparison of the firn model results using calculated (continuous lines) and measured (dashed lines) diffusion coefficient ratios (D_{gas}/D_{CO_2}) with FIRETRACC and CRYOSTAT data (symbols) for CFCs 11, 12 and 113. Colours are defined in Fig. 2, symbols are explained in Figs. 5 and 12 of the article.

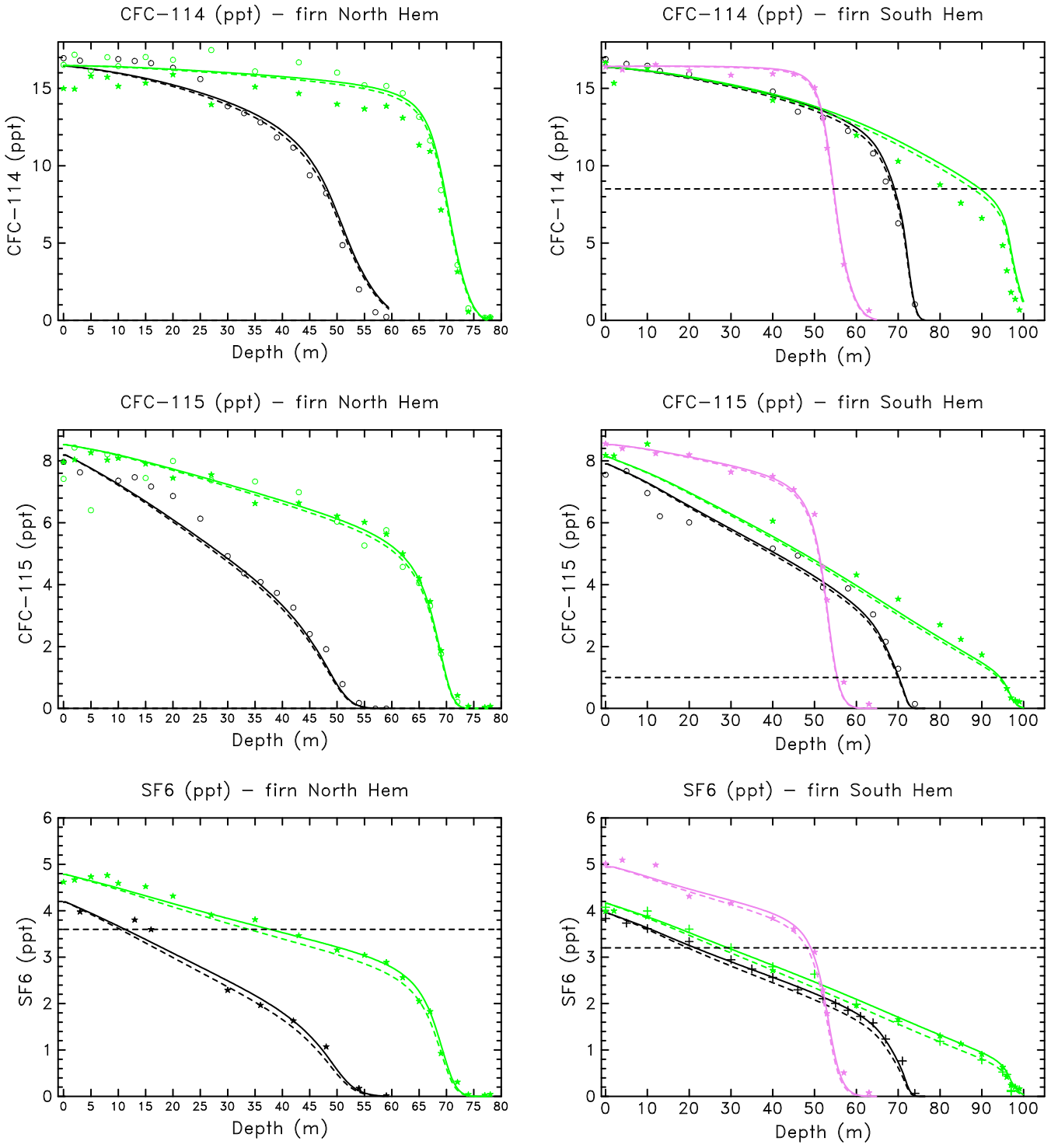

Fig. 4. Same as Fig. 3 for CFC-114, CFC-115 and SF_6.

Table 2. Width of CFC-11 age distribution: ages at (85% - 15%) accumulated probability (in years). c.o. stands for complete bubble close-off depth. We should note that North GRIP and Berkner ages at c.o.-0.2m are unreliable (see Sect. 5 of the article). Drill sites abbreviations: DI:Devon Island, NGR: North GRIP, BKN: Berkner Island, DML: Dronning Maud Land, DC: Dome C.

Distance to c.o.	DI	NGR	BKN	DML	DC
c.o. - 20m	21	15	10	18	29
c.o. - 15m	24	17	13	20	31
c.o. - 10m	28	22	32	24	33
c.o. - 5m	29	27	54	31	37
c.o. -0.2m	29	27	60	43	50

Table 3. Asymmetry of CFC-11 age distribution: (mean age - mode age)/(mean age) in percent. We should note that North GRIP and Berkner ages at c.o.-0.2m are unreliable (see Sect. 5 of the article).

Distance to c.o.	DI	NGR	BKN	DML	DC
c.o. - 20m	62	58	62	63	60
c.o. - 15m	52	51	56	57	54
c.o. - 10m	35	37	48	50	50
c.o. - 5m	20	14	27	35	44
c.o. -0.2m	14	10	16	10	24

ity and atmospheric trend estimates. Our atmospheric trends were calculated with an atmospheric chemistry model and are thus independent of the uncertainties on firn modelling. On the other hand, the Sturrock et al. (2002) trends were obtained by inverse firn modelling. Therefore calculated D_{gas}/D_{CO_2} ratios are used in this study in order to obtain a more consistent comparison with the Sturrock et al. (2002) trends.

4 Trace gas ages in firn

Figure 5 completes Fig. 7 of the article in illustrating the CFC-11 age distributions in the firn. These figures show results at 10 m depth intervals and selected measurement levels in the deepest part of the firn.

Site to site comparisons for the lower firn are made clearer by using the bubble close-off level (c.o.) as the reference depth. Tables 2 and 3 provide indicators of the width and asymmetry of age distributions at selected levels above full close-off depth. The following definitions are used in our age statistics: the mean age is the sum over time of ages multiplied by their probability at a given depth; the mode age is the age of maximum probability; and the median age is the age at 50% accumulated probability. For our distributions, the mode age is lower than the median age, which is lower than the mean age. The difference between 15% and 85% accumulated probability is close to a standard deviation (one sigma).

Table 4. Major characteristics of the firn physics.

	DI	NGR	BKN	DML	DC
Accu (cm/yr)	30	17	13	7	3.5
Temp (°C)	-23	-32	-26	-38	-53
c.o. depth (m)	59.6	78.2	65.0	76.4	100.2
c.o. width (m)	6	5	6	7	8
50yr sink (m)	18.5	10	7.5	4	2
Diffus surf	138	314	327	301	411
Diffus c.o.-20m	16.8	42.6	30.0	52.7	52.2
Diffus c.o.-5m	0.02	0.001	0.15	0.13	1.6

Several physical parameters may have an influence on age distributions in the firn.

The snow accumulation rate controls the sinking speed of the firn and thus the elimination of old air from the deepest firn levels by trapping in closed bubbles. In our model, most of the close-off process occurs in the last 5 to 8 meters. The close-off widths in Table 4 correspond to the depth interval in which the closed porosity over total porosity ratio goes from 10% to 100%. They should be compared to the firn sinking due to snow accumulation at the time scale of our study. This can be estimated simply as the time scale multiplied with the accumulation rate and divided by the firn density at close-off. ”50yr sink” values in Table 4 show that the firn sinking in 50 years is significant at all sites, and important at high accumulation sites.

On the other hand, both temperature and accumulation rate influence the snow metamorphism. High temperatures accelerate the transformation of snow into ice, whereas accumulation is related to snow burying, which implies higher pressure constraints and thus accelerated snow compaction. At our five sites, the firn thickness (”c.o. depth” in Table 4) appears more correlated to temperature than accumulation. However the North GRIP / DML comparison indicates that temperature is not the only influent parameter. In fact, its effect is probably more important at high temperatures (closer to the snow melting point).

Firn diffusivity is a complex parameter which depends not only on snow metamorphism but also on heterogeneities in firn, which may limit diffusivity. Devon Island firn, containing numerous refrozen melt layers, provides a good illustration of this effect by showing low diffusivities. Although there are variations with depth, diffusivities at our five sites look fairly correlated with the accumulation rate.

The width of age distributions increases with depth at all sites (Table 2), but this widening is much smaller at Arctic (high accumulation) than Antarctic (low accumulation) sites. The asymmetry of age distributions (Table 3) strongly decreases with depth at all sites. The relative difference between mean and mode age decreases from 58-63% at 20m

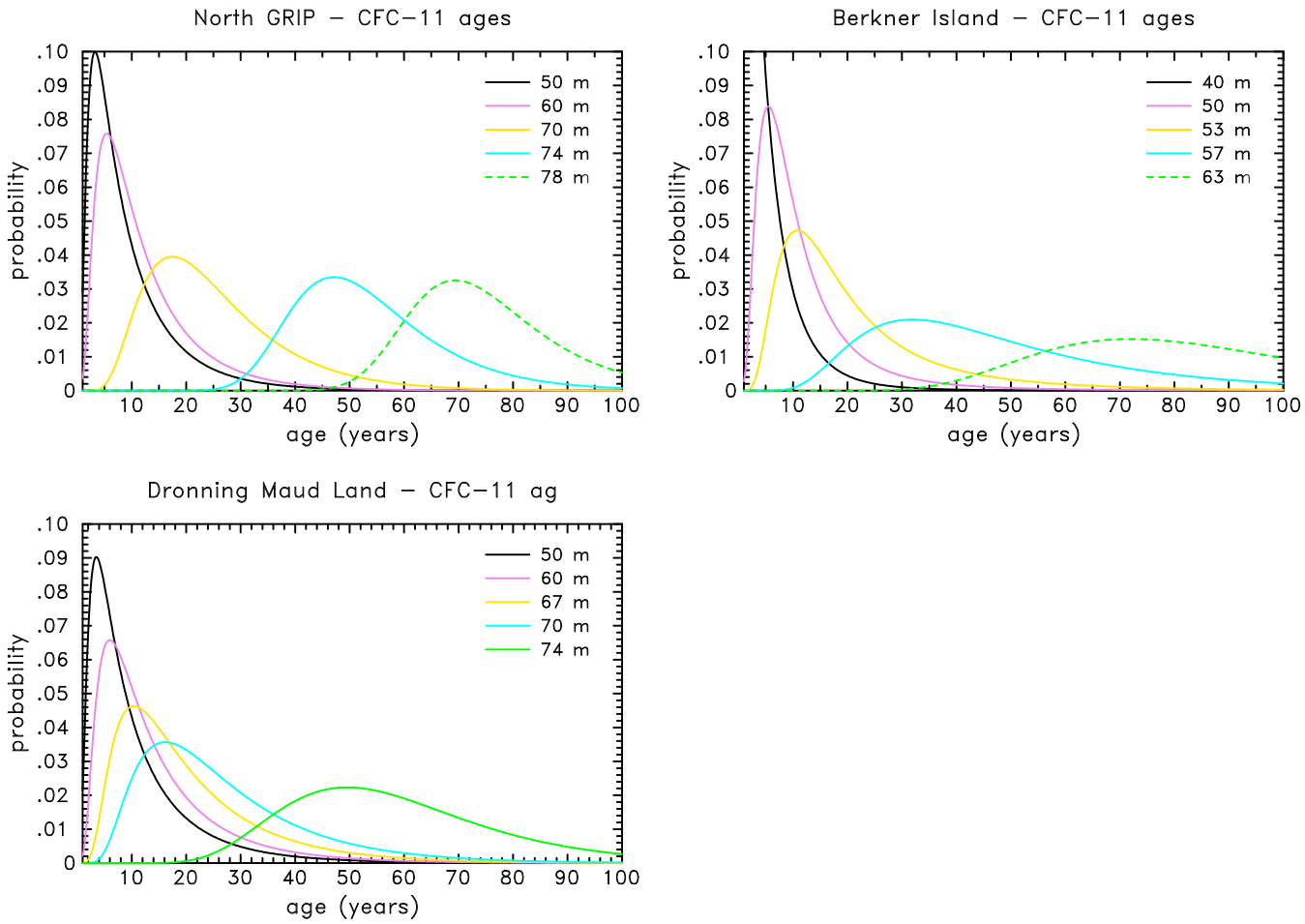

Fig. 5. CFC-11 age distributions at selected depths in the North GRIP, Berkner Island, and Dronning Maud Land firns. Dashed lines correspond to depth levels where firn model ages are inconsistent with ages calculated as the atmospheric scenario age corresponding to the measured concentration in firn (Table 3 of the article).

above close-off to 10-24% in the last model layer before full close-off. This decrease occurs at higher depths at Arctic sites than Antarctic sites. It may reflect a stronger influence of the close-off process which removes old air from the firn.

5 Recent trends in atmospheric concentrations

Table 5 presents the correction factors applied to emission inventories in order to fit the observed concentration trends. These corrections best fit the AGAGE record except for CCl_4, for which we fit the ESRL record which is more consistent with our firn data (UEA calibration scale), SF_6 (the AGAGE record is too recent for this gas) and CFCs 114 and 115 for which the only available long term trend was measured on the Cape Grim air archive. A constant correction factor always allows to fit the ascending part of the concentration record, which is dominated by the effect of emissions (see Sect. 6.4 of the article). However, different corrections often had to be applied in order to fit the recent stabilizing or decreasing parts of the concentration trends. As the effect of chemical losses becomes important at this time, the different corrections might be due to an error on the chemical losses.

Table 5. Correction factors on emissions used to fit the atmospheric concentration records.

Species	Emission correction
CFC-11	+6% before 1989; -7% between 1989 and 1995
CFC-12	+10% before 1990; -10% between 1990 and 1994
CFC-113	-7% before 1992; +20% between 1992 and 1996; +140% after 1996
CFC-114	+15% all the time
CFC-115	+5% all the time
CCl_4	+5% before 1994; +25% between 1994 and 2002
SF_6	+11% all the time

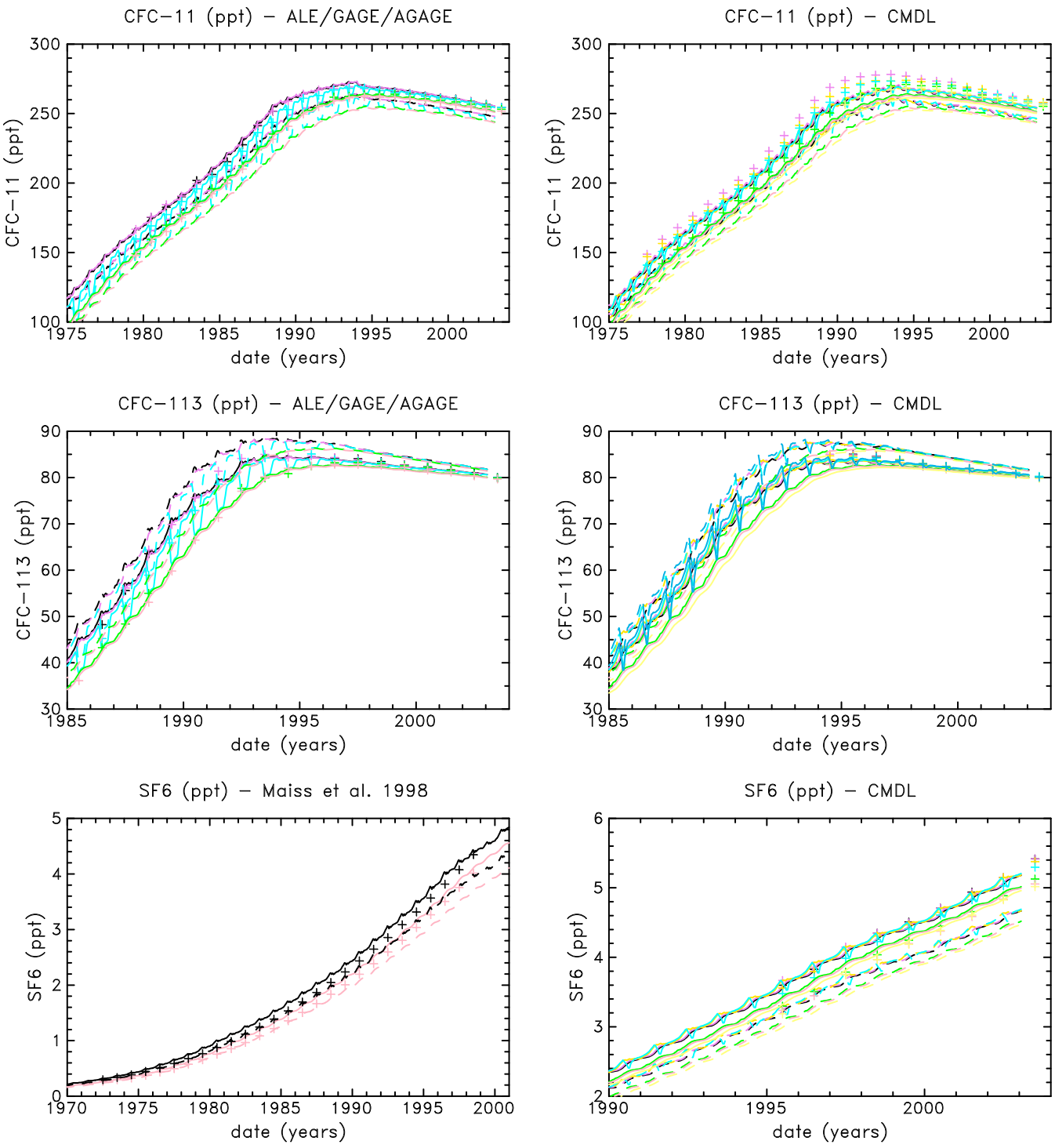

Fig. 6. Comparison of the chemistry model results (lines) for major CFCs with atmospheric data (plus signs). The different colours depict trends at ground level for different latitudes. Left panel: comparison with ALE/GAGE/AGAGE data: violet: Adrigole (52°N) and Mace Head (53°N), black: Oregon (45°N) and Trinidad Head (41°N), turquoise: Barbados (13°N), green: Samoa (14.3°S), pink: Cape Grim (40.7°S). Right panel: comparison with ESRL data: black: Alert (82.5°N), violet: Pt. Barrow (71.3°N), orange: Niwot Ridge (40.1°N), turquoise: Mauna Loa, Hawaii (19.5°N), blue: Cape Kumukahi, Hawaii (19.5°N), green: Samoa (14.3°S), pink: Cape Grim (40.7°S), yellow: South Pole (90°S). Dashed lines show model results obtained with unadjusted emission scenarios, whereas continuous lines show model results obtained with modified emissions to fit the ALE/GAGE/AGAGE records. For SF_6, emissions are adjusted to the ESRL record; Maiss and Brenninkmeijer (1998) data show a fit to Cape Grim measurements and a consistent best estimate of Northern Hemisphere concentrations.

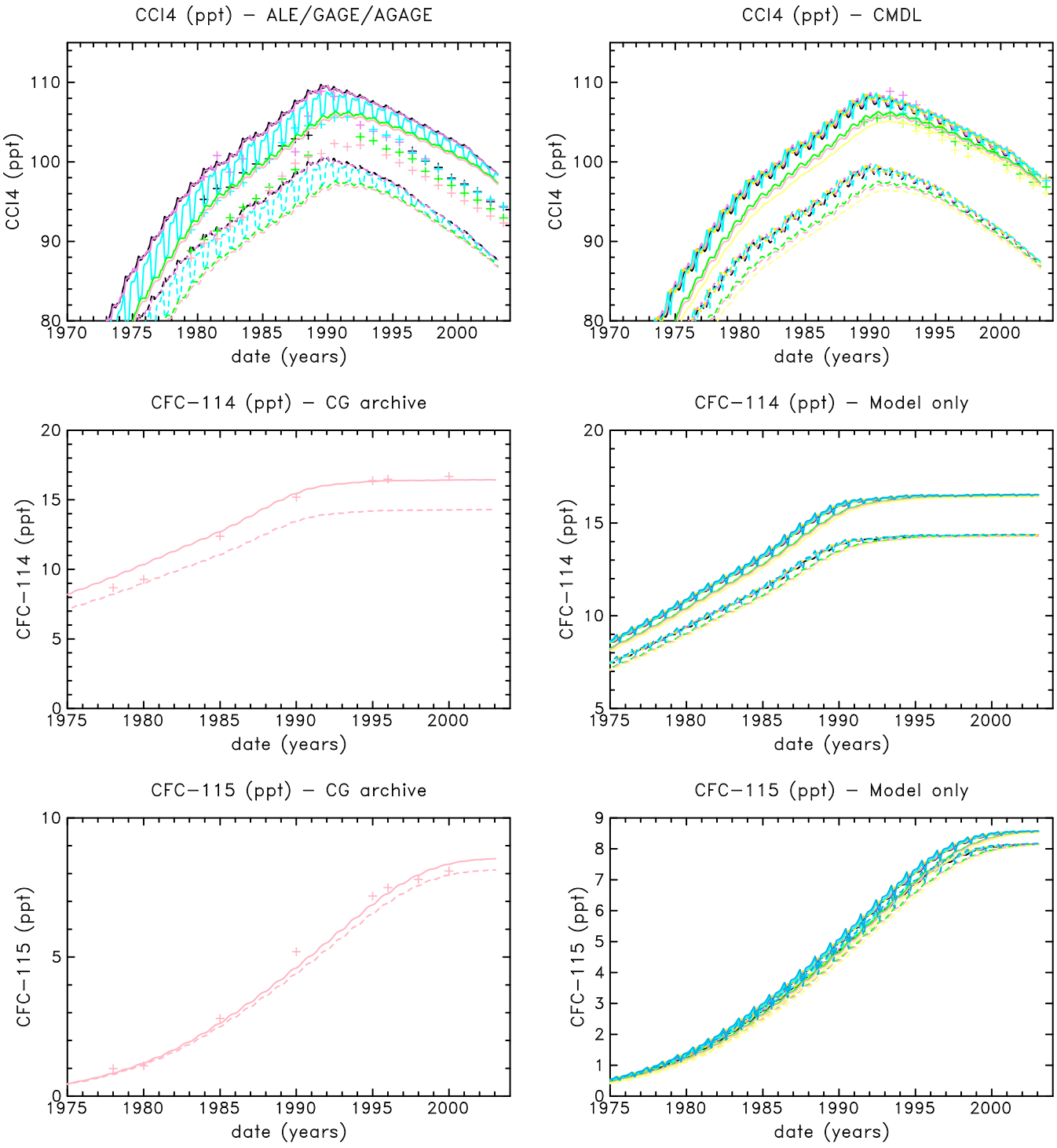

Fig. 7. Same as Fig. 6 except for continuous lines : CCl_4 emissions are adjusted to fit ESRL concentration data (this calibration scale is more consistent with the UEA data in firn); CFC-114 and CFC-115 emissions are adjusted to fit Cape Grim air archive data (from Fig 1.1 and Table 1.1 in WMO (2003), quoting Oram (1999)).

On the other hand, the nature of emissions also changed in the recent past, with contributions of non-reporting countries becoming dominant, and possibly some changes in major end uses and banking times of CFCs.

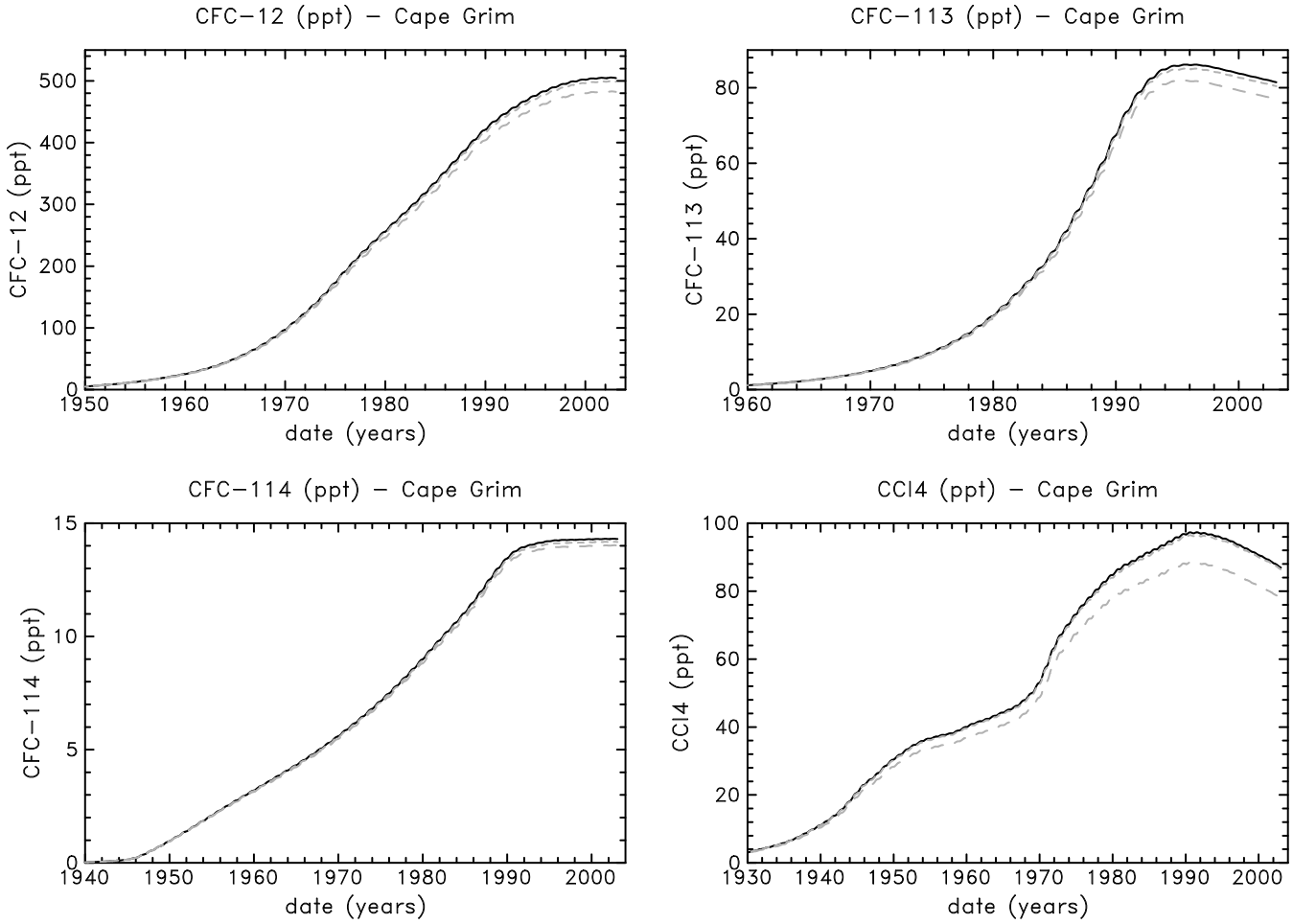

Fig. 8. Impact of spatial and temporal lifetime changes on halocarbon concentration trend. Continuous line: reference concentration trend. Long dashed line: concentration calculated with a constant and homogeneous lifetime (equilibrium lifetime). Short dashed line: concentration calculated when imposing the equilibrium lifetime as a scaling factor to the calculated halocarbon sink.

The negative corrections for CFC-11 and CFC-12 during the first half of the 1990's suggest that their emission reduction following the Montreal protocol may have been more efficient that expected. The very strong correction of CFC-113 emissions (+140%) is applied to very low values (about 2.5% of CFC-113 peak emissions). CFC-114 has the highest correction, and shows an even stronger calibration uncertainty as well as inconsistencies between data and model results in the firn, thus the budget of this species is poorly constrained. The emission correction is also high (11%) for SF_6, but Fig. 6 shows that a fit to ESRL data over-estimates Maiss and Brenninkmeijer (1998) data.

Fig. 6 and Fig. 7 complete Fig. 2 and Fig. 3 of the article. They confirm that meridional distributions of our target gases are well reproduced by the chemistry model. The reduced inter-hemispheric gradients in recent years due to the reduced (mostly in Northern hemisphere) emissions is also simulated. For CFC-11, SF_6 and CCl_4, model results which fit one plotted data set do not fit the other one. This indicates that there are inter-calibration differences between those data sets. Efforts have been made to reduce such differences and they have changed with time (WMO, 2007).

Over the most recent part of major CFC records (after 1995) the model correctly simulates the data slopes for CFC-11 and CFC-12, thus no correction needs to be applied. It is not the case for CFC-113, which has the most reduced emissions: model results decrease too fast. It could be due to a strong under-estimation of its emissions (by 140%). As chemical losses largely dominate emissions at that time (see Sect 6.4 of the article) a 40% reduction of its chemical losses during that period also fits the concentration data. Such a correction corresponds to a CFC-113 lifetime of 84 years instead of 71 years in 2002.

Our preferred emission scenario for SF_6 (see Sect. 2.1 of the article), corrected with a constant 11% increase, fit the slope reduction in concentration trend around 1998-2002 vis-

ible on the ESRL record as well as our firn air records. However it over-estimates Maiss and Brenninkmeijer (1998) data. An alternate emission scenario was tested, using the released sales data from Maiss and Brenninkmeijer (1998) between 1953 and 1990, "observed" emissions from Maiss and Brenninkmeijer (2000) between 1991 and 1996, and their linear extrapolation between 1997 and 2002. The two emission datasets are almost identical before 1990, but show opposite trends after 1995. The alternate emissions fit the Maiss and Brenninkmeijer (1998) data until 1985 without any correction but increasingly under-estimate them afterwards, they fit ESRL data in 2002 but under-estimates previous ESRL data, thus showing a too strong slope in 1995-2002. As mentionned in the article, this scenario also under-estimates near surface SF_6 concentrations at our three firn sites drilled in 1998-1999.

There are strong uncertainties on the CCl_4 budget. Fig. 7 shows an important inter-calibration difference between the AGAGE and ESRL records. On the other hand, the shape of the record is correctly simulated, suggesting that Simmonds et al. (1998) methodology of scaling CCl_4 emissions to CFC production is correct. An important correction factor had to be applied to fit the ESRL record after 1993 (25%), but the emissions are less than 20% of their peak value in that period. However, the recent inter-hemispheric gradient in CCl_4 concentration may be under-estimated by our model, suggesting somewhat stronger sources compensated by a sink efficient in both hemispheres.

Our CFC-115 model results are fairly consistent with the Cape Grim air archive record. CFC-114 shows higher discrepancies. Its emissions have to be increased by 15% in order to reach the recent CFC-114 observed concentration, and the concentration slope between 1978 and 1990 is underestimated by our chemistry model results.

6 Halocarbon lifetime tests

Fig. 8 completes Fig. 13 of the article. It illustrates the fact that the bias due to the use of homogeneous lifetimes rather than photochemical losses occuring only at high altitude is higher for relatively short lived species such as CCl_4 (or CFC-11) than for longer-lived species. The very long-lived CFC-115 is not plotted because the differences between our three test simulations are invisible for this compound. The even longer-lived SF_6 has insignificant losses at the time scale of our simulations.

References

Butler, J. H., Battle, M., Bender, M. L., Montzka, S. A., Clarke, A. D., Saltzman, E. S., Sucher, C. M., Severinghaus, J. P., and Elkins, J. W.: A record of atmospheric halocarbons during the twentieth century from polar firn air, Nature, 399, 749–755, 1999.

Bzowski, J., Kestin, J., Mason, E. A., and Uribe, F.: Equilibrium and transport properties of gas mixtures at low density: eleven polyatomic gases and five noble gases, J. Phys. Chem. Ref. Data, 19, 1179–1232, 1990.

CRYOSTAT: CRYOspheric STudies of Atmospheric Trends in stratospherically and radiatively important gases (CRYOSTAT), http://badc.nerc.ac.uk/data/cryostat, access: 31 July 2008, 2007.

Fabre, A., Barnola, J.-M., Arnaud, L., and Chappellaz, J.: Determination of gas diffusivity in polar firn: comparison between experimental measurements and inverse modeling, Geophys. Res. Lett., 27, 557–560, 2000.

FIRETRACC: Firn Record of Trace Gases Relevant to Atmospheric Chemical Change over 100 yrs (FIRETRACC/100), http://badc.nerc.ac.uk/data/firetracc, access: 31 July 2008, 2007.

Fuller, E. N., Schettler, P. D., and Giddings, J. C.: A new method for prediction of binary gas-phase diffusion coefficients, Ind. Eng. Chem., 58, 19–27, doi:10.1021//ie50677a007, 1966.

Gilliland, E. R.: Diffusion coefficients in gaseous systems, Ind. Engng. Chem., 26, 681–685, 1934.

Le Bas, G.: The molecular volumes of liquid chemical compounds, Longmans, London, UK, 1915.

MacFarling Meure, C., Etheridge, D., Trudinger, C., Steele, P., Langenfelds, R., van Ommen, T., Smith, A., and Elkins, J.: Law Dome CO_2, CH_4 and N_2O ice core records extended to 2000 years BP, Geophys. Res. Lett., 33, L14 810, doi:10.1029/2006GL026152, 2006.

Maiss, M. and Brenninkmeijer, C. A. M.: Atmospheric SF_6: Trends, Sources, and Prospects, Environ. Sci. Technol., 32, 3077–3086, 1998.

Maiss, M. and Brenninkmeijer, C. A. M.: A reversed trend in emissions of SF_6 into the atmosphere?, in: Non CO_2 greenhouse gases: scientific understanding, control and implementation, Proc. 2nd international symp., edited by Ham, J. V., Baede, A. P. M., Meyer, L. A., and Ybema, R., pp. 199–204, Kluwer Academic Publishers, Dordrecht, Noordwijkerhout, The Netherlands, 2000.

Marrero, T. R. and Mason, E. A.: Gaseous diffusion coefficients, J. Phys. Chem. Ref. Data, 1, 3–118, 1972.

Matsunaga, N., Hori, M., and Nagashima, A.: Mutual diffusion coefficients of halogenated-hydrocarbon refrigerant - air systems, High Temperatures High Pressures, 25, 63–70, 1993.

Matsunaga, N., Hori, M., and Nagashima, A.: Diffusion coefficients of global warming gases into air and its component gases, High Temperatures High Pressures, 30, 77–83, 1998.

Matsunaga, N., Hori, M., and Nagashima, A.: Measurements of the mutual diffusion coefficients of gases by the Taylor method (7th Report, measurements on the SF_6-air, SF_6-N_2, SF_6-O_2, CFC12-N_2, CFC12-O_2, HCFC22-N_2 and HCFC22-O_2 systems), Trans. Jpn. Soc. Mech. Eng. B., 68, 550–555, 2002.

Oram, D. E.: Trends of long-lived anthropogenic halocarbons in the Southern Hemisphere and model calculations of global emissions, Ph.D. thesis, University of East Anglia, Norwich, U.K., 1999.

Perry, R. H. and Chilton, C. H.: Chemical engineers handbook, 5th ed., McGraw-Hill, New York, USA, 1973.

Rommelaere, V.: Trois problèmes inverses en glaciologie., Ph.D. thesis, Université Joseph Fourier, Grenoble, France, 1997.

Rommelaere, V., Arnaud, L., and Barnola, J.-M.: Reconstructing recent atmospheric trace gas concentrations from polar firn and

bubbly ice data by inverse methods, J. Geophys. Res., 102, 30 069–30 083, 1997.

Simmonds, P. G., Cunnold, D. M., Weiss, R. F., Prinn, R. G., Fraser, P. J., McCulloch, A., Alyea, F. N., and O'Doherty, S.: Global trends and emission estimates of CCl_4 from in situ background observations from July 1978 to June 1996, J. Geophys. Res., 103, 16 107–16 027, 1998.

Sturges, W. T., Wallington, T. J., Hurley, M. D., Shine, K. P., Sihra, K., Engel, A., Oram, D. E., Penkett, S. A., Mulvaney, R., and Brenninkmeijer, C. A. M.: A Potent Greenhouse Gas Identified in the Atmosphere: SF_5CF_3, Science, 289, 611–613, 2000.

Sturrock, G. A., Etheridge, D. M., Trudinger, C. M., Fraser, P. J., and Smith, A. M.: Atmospheric histories of halocarbons from analysis of Antarctic firn air: Major Montreal Protocol species, J. Geophys. Res., 107, 4765, doi:10.1029/2002JD002548, 2002.

Trudinger, C. M., Enting, I. G., Etheridge, D. M., Francey, R. J., Levchenko, V. A., and Steele, L. P.: Modeling air movement and bubble trapping in firn, J. Geophys. Res., 102, 6747–6763, 1997.

Trudinger, C. M., Etheridge, D. M., Rayner, P. J., Enting, I. G., Sturrock, G. A., and Langenfelds, R. L.: Reconstructing atmospheric histories from measurements of air composition in firn, J. Geophys. Res., 107, 4780, doi:10.1029/2002JD002545, 2002.

Wilke, C. R. and Lee, C. Y.: Estimation of diffusion coefficients for gases and vapors, Ind. Eng. Chem., 47, 1253–1257, doi:10.1021/ie50546a056, 1955.

WMO: Scientific Assessment of Ozone Depletion: 2002, Global Ozone Research and Monitoring Project, Report No.47, World Meteorological Organization, Geneva, 2003.

WMO: Scientific Assessment of Ozone Depletion: 2006. Global Ozone Research and Monitoring Project - Report No.50, World Meteorological Organization, Geneva, http://ozone.unep.org/Publications, 2007.